Electronic Supplementary Material (ESI) for Physical Chemistry Chemical Physics.

Supporting Information:

The key to the yellow-to-cyan tuning in the green fluorescent protein family is polarisation

Riccardo Nifosì,*,† Benedetta Mennucci,‡ and Claudia Filippi¶

†*NEST, CNR-Istituto Nanoscienze and Scuola Normale Superiore, Piazza San Silvestro 12, 56127 Pisa, Italy*

‡*Dipartimento di Chimica e Chimica Industriale, Universitaà di Pisa, Via Giuseppe Moruzzi 13, 56124 Pisa, Italy*

¶*MESA+ Institute for Nanotechnology, University of Twente, P.O. Box 217, 7500 AE Enschede, The Netherlands*

E-mail: riccardo.nifosi@nano.cnr.it

S1 Structural models

In our models the QM subsystem includes the chromophore capped as in Fig. S1 and, when present, the π-stacked residue. The QM subsystem is optimised by DFT with PBE0 functional and the 6-31G(d) basis set, resulting in changes from the starting X-ray structure shown in Fig. S2.

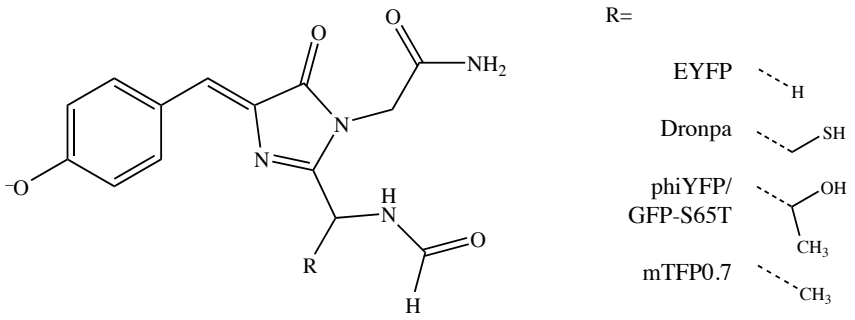

Figure S1: QM model of the chromophore.

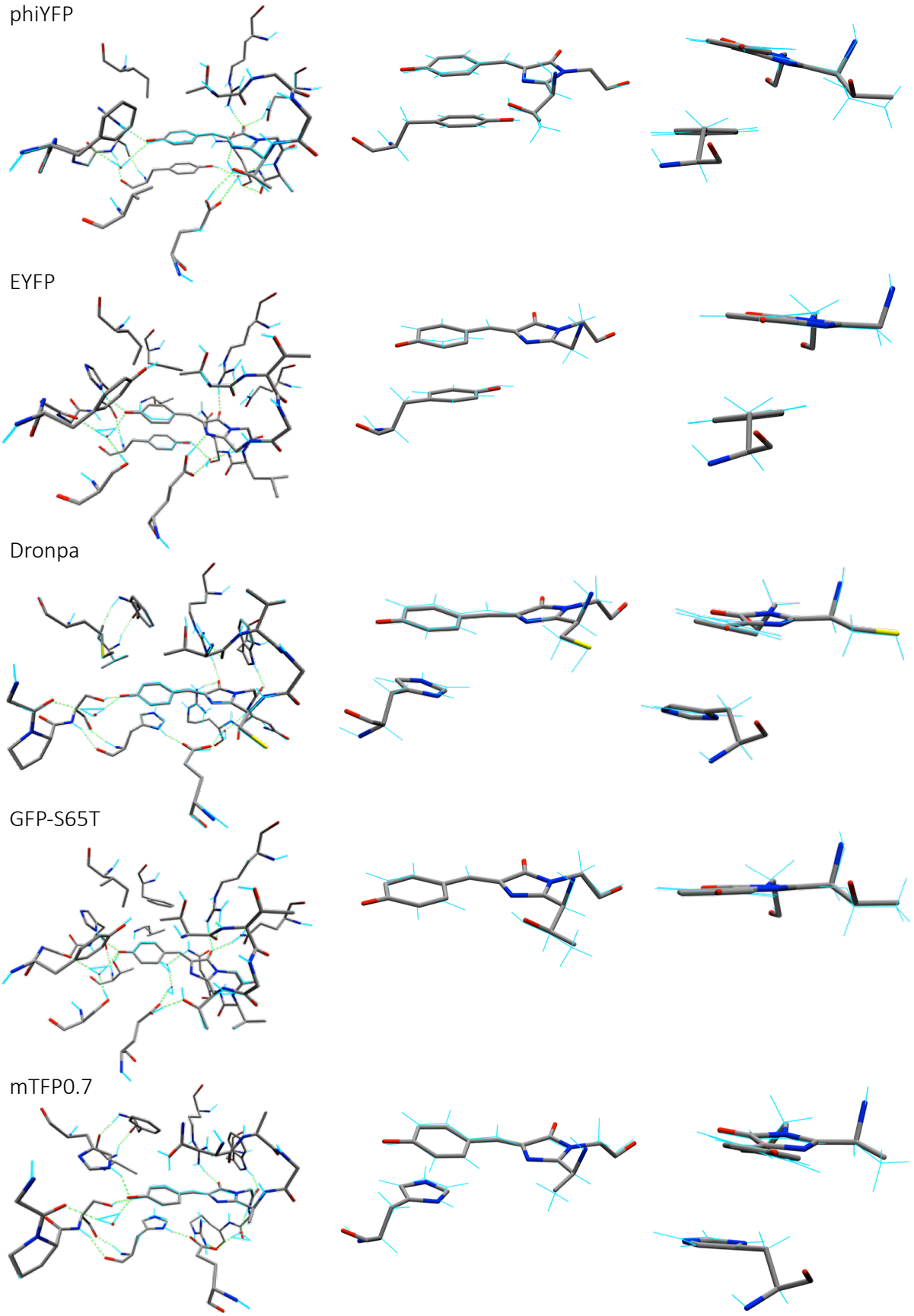

Figure S2: Comparison between the final QM-optimized models (cyan lines) and the starting X-ray structures ("licorice" atom-color representation). For EYFP and GFP-S65T, only the $OH^{145}\uparrow$ models are shown.

Excitation energies for different QM subsystems

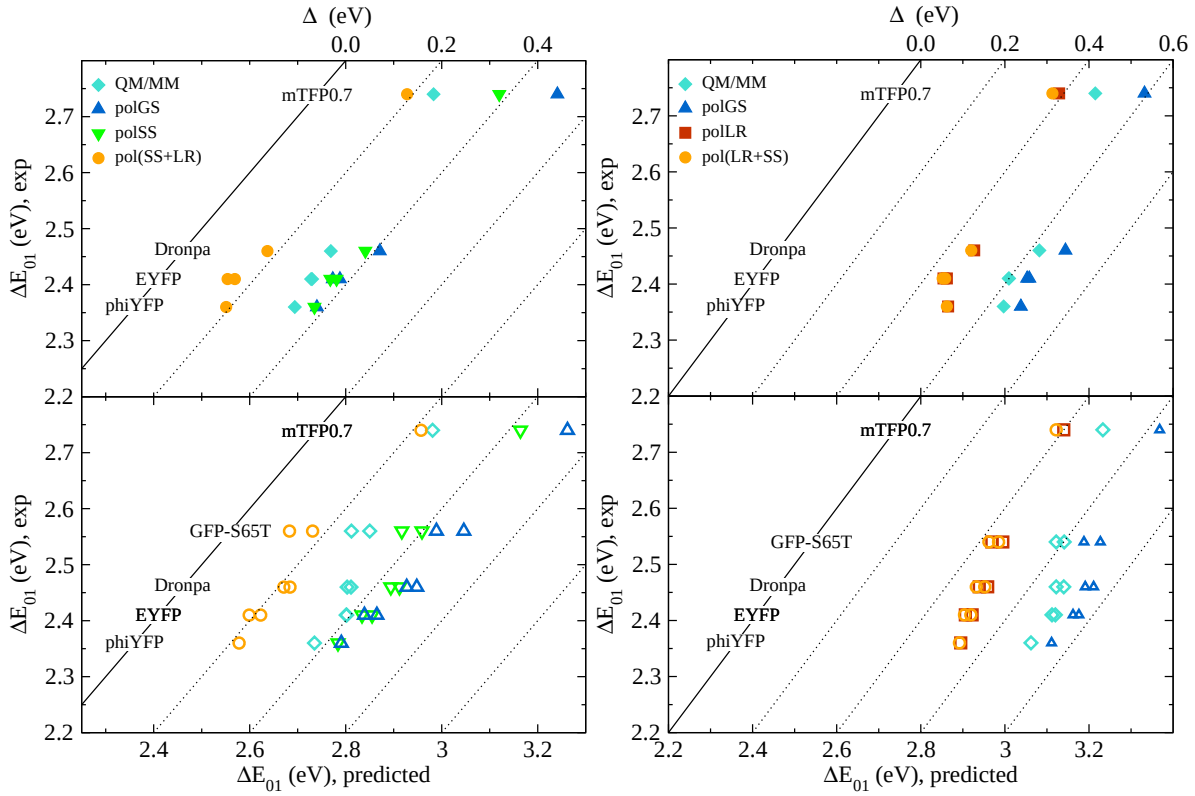

Figure S3: Left: CASPT2 excitation energies computed with only the chromophore as QM part (bottom panel, hollow symbols) and with the chromophore plus the π-stacked residue as QM (top panel, filled symbols). Right: same as Left with TD-DFT/CAM-B3LYP.

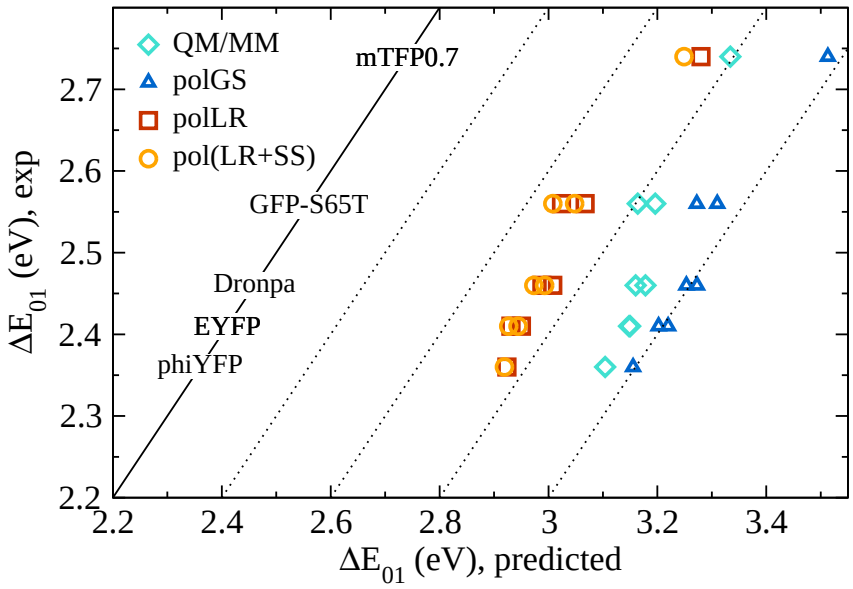

Figure S4: Same as left panel of Figure S3 with TD-DFT/LC-BLYP. The calculations employ only the chromophore as QM subsystem.

Table S1: CASSCF and CASPT2 excitation energies (eV) computed with the chromophore and the chromophore plus the π-stacked residue as QM subsystem.

Protein	CASSCF			CASPT2		
	$\Delta E_{01}^{\mathrm{QM/MM}}$	$\Delta E_{01}^{\mathrm{polGS}}$	$\Delta E_{01}^{\mathrm{polSS}}$	$\Delta E_{01}^{\mathrm{QM/MM}}$	$\Delta E_{01}^{\mathrm{polGS}}$	$\Delta E_{01}^{\mathrm{polSS}}$
QM subsystem: chromophore						
phiYFP	3.159	3.188	3.180	2.735	2.791	2.784
EYFP $OH^{145}\uparrow$	3.236	3.225	3.220	2.802	2.840	2.836
EYFP $OH^{145}\downarrow$	3.220	3.252	3.239	2.801	2.865	2.855
Dronpa (2iov)	3.232	3.381	3.334	2.811	2.948	2.912
Dronpa (2z1o)	3.222	3.358	3.314	2.803	2.927	2.894
GFP-S65T $OH^{145}\uparrow$	3.211	3.487	3.390	2.812	2.989	2.917
GFP-S65T $OH^{145}\downarrow$	3.270	3.607	3.481	2.850	3.046	2.959
mTFP0.7	3.458	3.982	3.799	2.981	3.262	3.164
QM subsystem: chromophore + π-stacked residue						
phiYFP	3.144	3.161	3.157	2.694	2.740	2.735
EYFP $OH^{145}\uparrow$	3.189	3.186	3.180	2.730	2.773	2.768
EYFP $OH^{145}\downarrow$	3.171	3.205	3.195	2.728	2.788	2.781
Dronpa (2z1o)	3.205	3.316	3.280	2.769	2.871	2.841
mTFP0.7	3.480	3.991	3.805	2.983	3.241	3.120

Table S2: TD-DFT/CAM-B3LYP excitation energies (eV) and transition dipole moments (Debye) computed with the chromophore and the chromophore plus the π-stacked residue as QM subsystem. We also report the TD-DFT/LC-BLYP results with only the QM chromophore.

Protein	QM/MM		polLR			
	ΔE_{01}	μ_{01}	$\Delta E_{01}^{\mathrm{polLR}}$	μ_{01}	$\Delta E_{01}^{\mathrm{polGS}}$	$\Delta E_{01}^{\mathrm{pol(LR+SS)}}$
CAM-B3LYP						
QM subsystem: chromophore						
phiYFP	3.062	9.639	2.895	10.750	3.111	2.892
EYFP $OH^{145}\uparrow$	3.112	9.975	2.908	11.030	3.163	2.906
EYFP $OH^{145}\downarrow$	3.120	9.955	2.922	10.997	3.176	2.919
Dronpa (2iov)	3.140	9.686	2.959	10.684	3.211	2.952
Dronpa (2z1o)	3.122	9.763	2.939	10.783	3.191	2.932
GFP-S65T $OH^{145}\uparrow$	3.122	9.537	2.969	10.503	3.205	2.962
GFP-S65T $OH^{145}\downarrow$	3.141	9.460	2.995	10.404	3.227	2.985
mTFP0.7	3.233	9.305	3.140	10.113	3.368	3.122
QM subsystem: chromophore + π-stacked residue						
phiYFP	2.997	9.038	2.865	10.175	3.038	2.862
EYFP $OH^{145}\uparrow$	3.010	8.952	2.854	10.178	3.053	2.852
EYFP $OH^{145}\downarrow$	3.009	8.833	2.862	10.090	3.058	2.858
Dronpa (2z1o)	3.082	9.426	2.927	10.466	3.144	2.920
mTFP0.7	3.215	9.043	3.129	9.915	3.332	3.113
LC-BLYP						
QM subsystem: chromophore						
phiYFP	3.104	9.934	2.924	10.983	3.155	2.919
EYFP $OH^{145}\uparrow$	3.150	10.252	2.931	11.246	3.202	2.927
EYFP $OH^{145}\downarrow$	3.157	10.224	2.950	11.195	3.220	2.944
Dronpa (2iov)	3.178	9.950	3.008	10.842	3.273	2.993
Dronpa (2z1o)	3.160	10.030	2.988	10.949	3.253	2.973
GFP-S65T $OH^{145}\uparrow$	3.164	9.776	3.024	10.635	3.272	3.008
GFP-S65T $OH^{145}\downarrow$	3.196	9.671	3.067	10.503	3.310	3.048
mTFP0.7	3.334	9.444	3.280	10.111	3.513	3.249

S2 Polarization contributions to ΔE and dipole moments

Table S3: TD-DFT/CAM-B3LYP polLR and CASPT2 polSS contributions (eV). The polLR CASPT2 corrections (Δ^{LR}) are estimated as discussed in the main text (Eq. 2).

Protein	TD-DFT	CASPT2			
	Δ^{LR}	Δ^{SS}	$\mu_{01}^{\mathrm{polGS}}$	Δ^{LR}	$\Delta E_{01}^{\mathrm{pol(SS+LR)}}$
QM subsystem: chromophore					
phiYFP	-0.217	-0.007	10.486	-0.206	2.578
EYFP $OH^{145}\uparrow$	-0.257	-0.005	10.575	-0.235	2.599
EYFP $OH^{145}\downarrow$	-0.254	-0.010	10.512	-0.232	2.623
Dronpa (2iov)	-0.252	-0.036	10.154	-0.228	2.684
Dronpa (2z1o)	-0.252	-0.033	10.157	-0.224	2.671
GFP-S65T $OH^{145}\uparrow$	-0.236	-0.072	10.450	-0.234	2.683
GFP-S65T $OH^{145}\downarrow$	-0.232	-0.088	10.297	-0.227	2.731
mTFP0.7	-0.228	-0.098	9.645	-0.207	2.957
QM subsystem: chromophore + π-stacked system					
phiYFP	-0.174	-0.005	10.480	-0.184	2.551
EYFP $OH^{145}\uparrow$	-0.199	-0.006	10.541	-0.213	2.554
EYFP $OH^{145}\downarrow$	-0.197	-0.007	10.470	-0.212	2.569
Dronpa (2z1o)	-0.217	-0.030	10.154	-0.204	2.637
mTFP0.7	-0.203	-0.121	9.653	-0.193	2.928

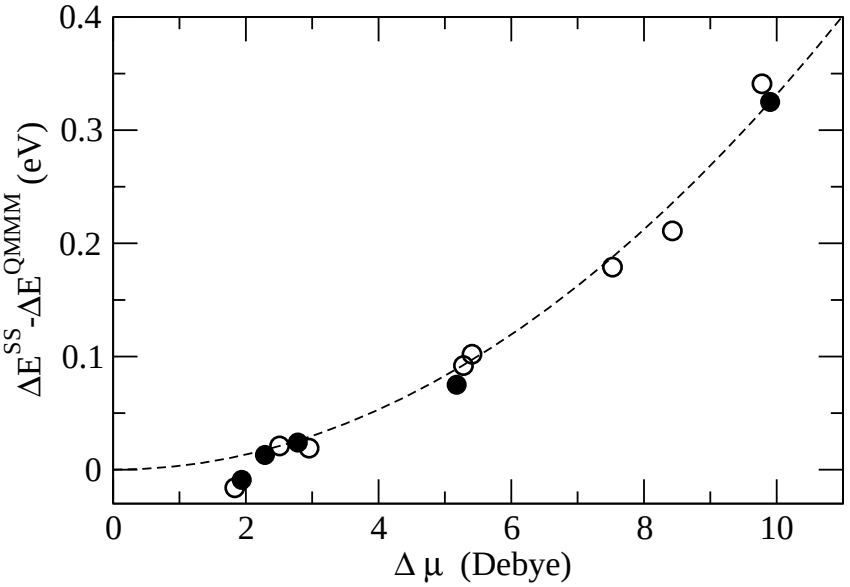

Figure S5: $\Delta\Delta E = \Delta E_{01}^{\mathrm{polSS}} - \Delta E_{01}^{\mathrm{QMMM}}$ plotted versus the $\Delta\mu^{\mathrm{polGS}}$ and computed at the CASSCF level (open circles: chromophore QM subsystem; solid circles: chromophore + π-stacked residue as QM subsystem). The quadratic coefficient from the fit is 0.0033 eV/Debye^2.

Table S4: TD-DFT dipole moment differences ($|\Delta\mu|$, Debye) in the various embedding schemes.

Protein	$\|\Delta\mu\|$ CAM-B3LYP		LC-BLYP	
	QM/MM	polGS	QM/MM	polGS
QM subsystem: chromophore				
phiYFP	0.888	1.690	0.668	2.221
EYFP $OH^{145}\uparrow$	0.482	1.492	0.177	2.017
EYFP $OH^{145}\downarrow$	0.677	1.774	0.563	2.457
Dronpa (2iov)	1.034	2.526	1.493	3.580
Dronpa (2z1o)	1.085	2.563	1.516	3.692
GFP-S65T $OH^{145}\uparrow$	1.331	2.627	1.783	3.777
GFP-S65T $OH^{145}\downarrow$	1.698	2.984	2.383	4.242
mTFP0.7	2.554	3.971	3.523	5.186
QM subsystem: chromophore + π-stacked system				
phiYFP	1.173	1.735	-	-
EYFP $OH^{145}\uparrow$	0.964	1.609	-	-
EYFP $OH^{145}\downarrow$	1.347	2.004	-	-
Dronpa (2z1o)	1.385	2.624	-	-
mTFP0.7	2.687	3.936	-	-

Table S5: CASSCF dipole moment differences ($|\Delta\mu|$, Debye) in the various embedding schemes, calculated either as the expectation value of the dipole operator $|\Delta\langle\Phi|\mu|\Phi\rangle|$ or by Finite Field Perturbation Theory (see Methods section in the main text).

Protein	$\|\Delta\langle\Phi\|\mu\|\Phi\rangle\|$			$\|\Delta\mu\|$ FFPT		
	QM/MM	polGS	polSS	QM/MM	polGS	polSS
QM subsystem: chromophore						
phiYFP	0.96	2.51	2.56	1.16	2.62	2.64
EYFP $OH^{145}\uparrow$	2.01	1.83	1.85	2.46	1.78	1.78
EYFP $OH^{145}\downarrow$	1.02	2.95	2.98	-	3.05	3.04
Dronpa (2iov)	1.24	5.41	5.63	1.22	6.06	6.10
Dronpa (2z1o)	1.45	5.28	5.46	1.47	5.88	5.91
GFP-S65T $OH^{145}\uparrow$	3.04	7.53	7.98	3.14	8.66	8.96
GFP-S65T $OH^{145}\downarrow$	4.68	8.43	9.10	4.99	9.80	10.36
mTFP0.7	6.93	9.78	11.19	7.68	11.88	13.07
QM subsystem: chromophore + π-stacked residue						
phiYFP	0.84	2.00	2.09	-	1.97	2.04
EYFP $OH^{145}\uparrow$	1.62	1.94	2.00	-	1.55	1.65
EYFP $OH^{145}\downarrow$	0.63	2.78	2.89	-	2.56	2.67
Dronpa (2z1o)	2.29	5.18	5.39	-	5.51	5.63
mTFP0.7	7.31	9.90	11.35	-	11.69	13.08

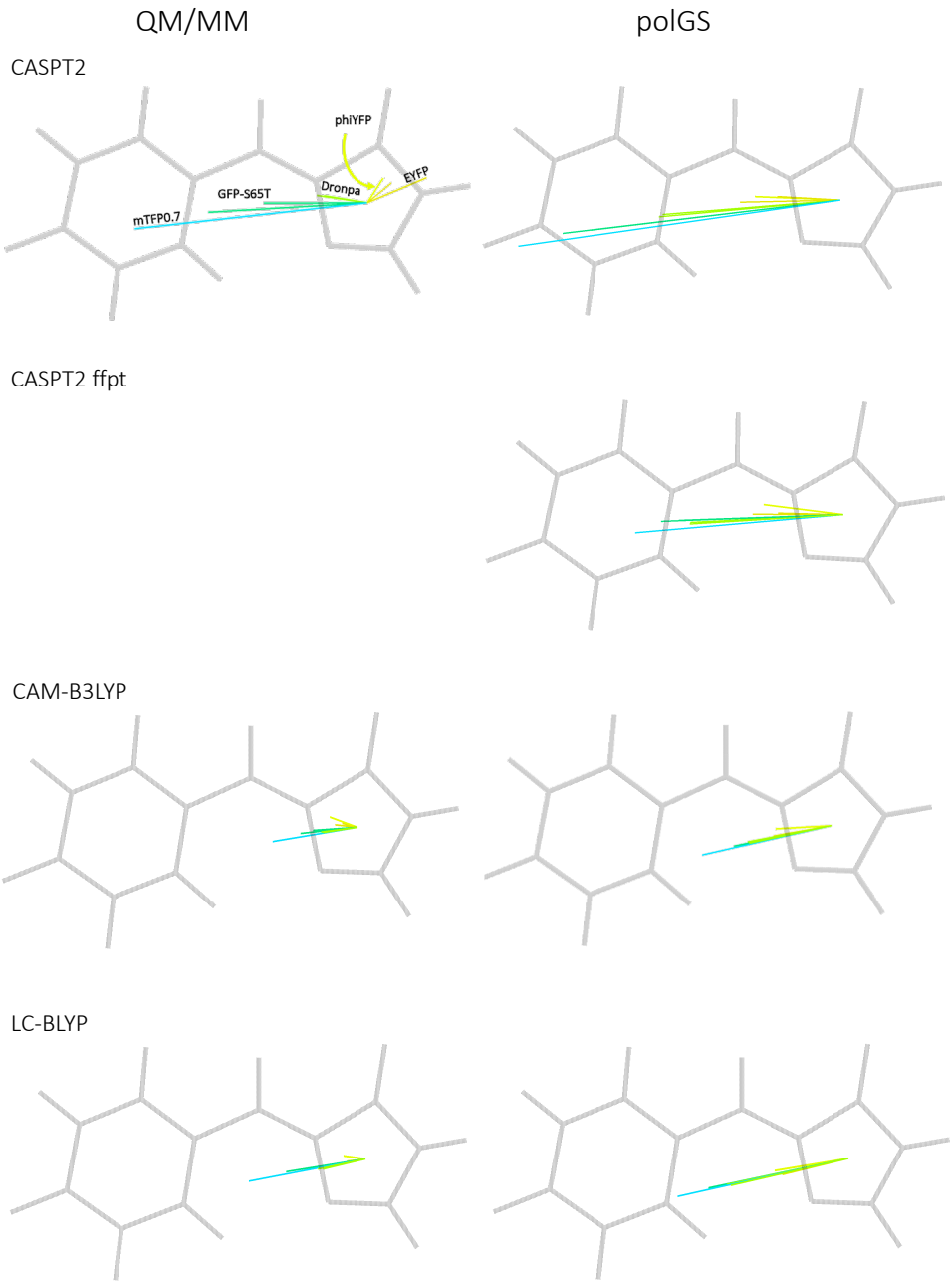

Figure S6: Comparison of direction and strength of CASPT2 and TD-DFT $\Delta\vec{\mu}$ in the various proteins and methods.

Table S6: CASPT2 $\Delta\mu$ in the various embedding schemes, calculated either as the expectation value of the dipole operator $|\Delta\langle\Phi|\mu|\Phi\rangle|$ or by Finite Field Perturbation Theory (see Methods section in the main text). The column MM reports the dipole contribution of the MM part (i.e. the vector sum of the $\Delta\mu$ for each MM site). The subsequent column lists its (vector) sum to the $\Delta\mu^{\mathrm{polSS}}$ value, namely, $|\Delta\vec{\mu}^{\mathrm{polSS}} + \Delta\vec{\mu}^{\mathrm{MM}}|$.

	$\lvert\Delta\langle\Phi\lvert\mu\rvert\Phi\rangle\rvert$			$\lvert\Delta\mu\rvert$ FFPT				
	QM/MM	polGS	polSS	QM/MM	polGS	polSS	MM	|polSS+MM|
QM subsystem: chromophore								
phiYFP	0.86	2.52	2.58	0.88	2.37	2.68	0.58	2.12
EYFP $OH^{145}\uparrow$	1.89	1.86	1.88	0.61	1.93	2.03	0.49	1.55
EYFP $OH^{145}\downarrow$	0.93	2.96	3.00	-	2.67	2.89	0.76	2.13
Dronpa (2iov)	1.28	5.39	5.64	3.60	4.54	4.99	1.34	3.68
Dronpa (2z1o)	1.49	5.27	5.46	2.44	4.52	5.09	1.35	3.58
GFP-S65T $OH^{145}\uparrow$	3.02	7.40	7.91	2.65	4.85	5.30	1.70	3.60
GFP-S65T $OH^{145}\downarrow$	4.64	8.27	9.00	3.78	5.39	6.12	1.95	4.17
mTFP0.7	6.83	9.62	11.09	5.48	6.17	7.63	2.48	5.15
QM subsystem: chromophore + π-stacked residue								
phiYFP	0.72	2.06	2.12	-	2.16	2.49	0.43	2.06
EYFP $OH^{145}\uparrow$	1.49	2.03	2.09	-	2.00	3.85	0.48	1.93
EYFP $OH^{145}\downarrow$	0.53	2.80	2.95	-	2.43	2.75	0.65	2.11
Dronpa (2z1o)	2.30	5.12	5.44	-	4.38	4.70	1.27	3.49
mTFP0.7	7.22	9.88	11.21	-	6.15	7.82	2.38	5.54

S3 Per-residue analysis

In TD-DFT, the per-residue contributions to the Δ^{LR} and Δ^{polSS}, reported in Fig. S7, can be defined as following:

$$E_i^{\mathrm{polGS}} = -\frac{1}{2}\sum_{a\in i}\vec{\mu}_a(\rho^{\mathrm{polGS}})\cdot\vec{F}_a^{\mathrm{chro}}(\rho_{\mathrm{polGS}}) \quad \text{(S1)}$$

$$\Delta_i^{\mathrm{LR}} = -\sum_{a\in i}\vec{\mu}_a(\rho_{01})\cdot\vec{F}_a^{\mathrm{chro}}(\rho_{01}) \quad \text{(S2)}$$

$$\Delta_i^{\mathrm{SS}} = -\frac{1}{2}\sum_{a\in i}\vec{\mu}_a(\Delta\rho)\cdot\vec{F}_a^{\mathrm{chro}}(\Delta\rho) \quad \text{(S3)}$$

where the sums run over the MM atoms in each protein residue. The quantities $\vec{\mu}_a(\rho^{GS})$, $\vec{\mu}_a(\rho_{01})$ and $\vec{\mu}_a(\Delta\rho)$ are the (MM) dipoles polarised, respectively, to the ground state density of the QM subsystem ρ^{polGS}, to its transition density ρ_{01}, and to the variation of electronic density upon excitation $\Delta\rho = \rho^{\mathrm{polES}} - \rho^{\mathrm{polGS}}$. $\vec{F}_a^{\mathrm{chro}}$ is the electric field at the MM site a, due to the corresponding density.

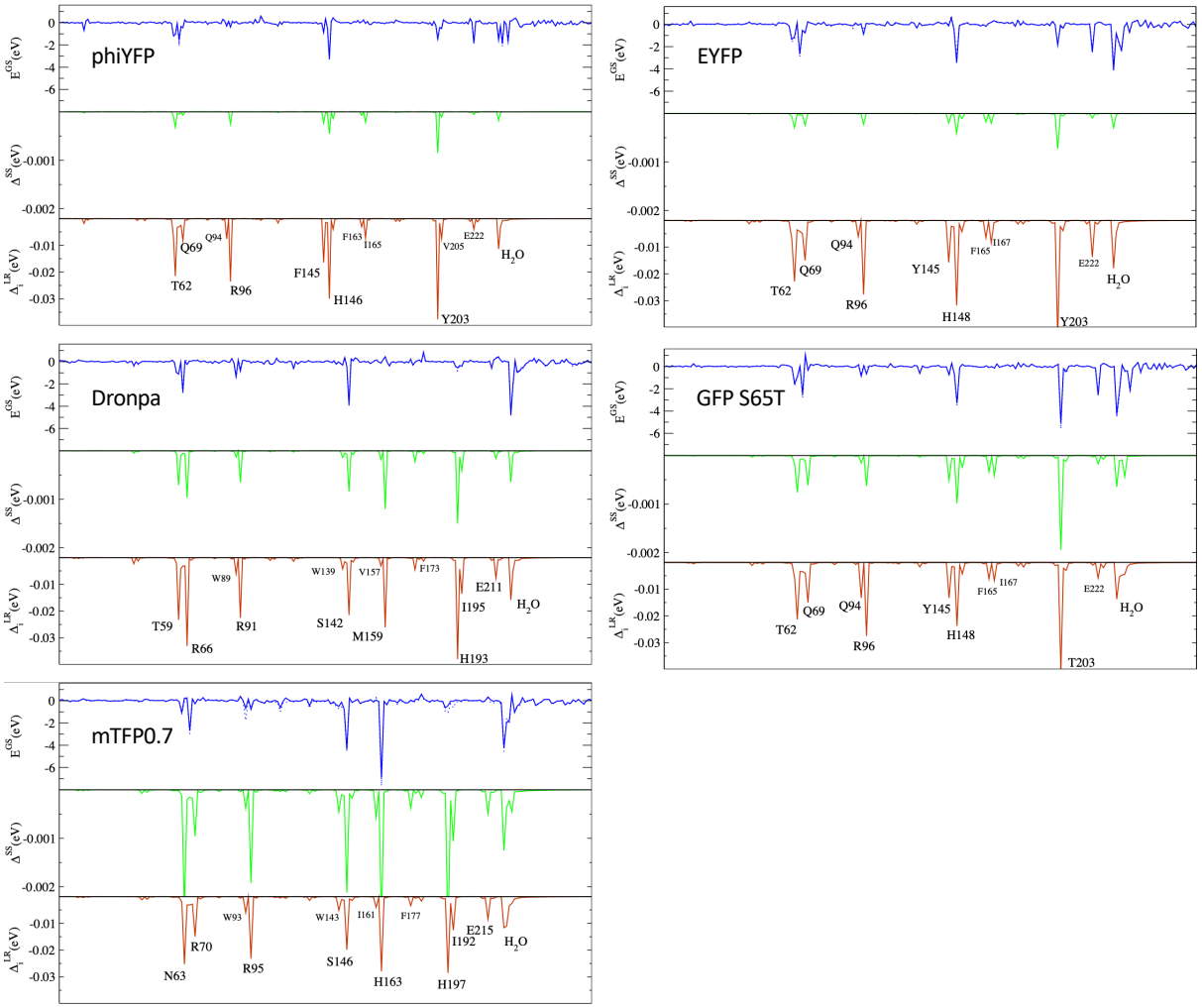

Figure S7: Per residue contributions to the ground-state DFT polarisation energy (E^{polGS}) and relative Δ^{LR} and Δ^{SS} contributions from TD-DFT/CAM-B3LYP calculations. The dotted blue line is the E^{polGS} contribution calculated at the CASSCF level.

Table S7: CASSCF and CASPT2 excitation energies (eV) of mTFP0.7 with selected residues removed from the model. The complete model (mTFP0.7) is reported again for the sake of comparison.

Model	CASSCF			CASPT2		
	$\Delta E_{01}^{\mathrm{QM/MM}}$	$\Delta E_{01}^{\mathrm{polGS}}$	$\Delta E_{01}^{\mathrm{polSS}}$	$\Delta E_{01}^{\mathrm{QM/MM}}$	$\Delta E_{01}^{\mathrm{polGS}}$	$\Delta E_{01}^{\mathrm{polSS}}$
QM subsystem: chromophore						
mTFP0.7	3.458	3.982	3.799	2.981	3.262	3.164
mTFP0.7 -W1	3.372	3.727	3.610	2.916	3.166	3.101
mTFP0.7 -S146	3.354	3.735	3.607	2.902	3.175	3.093
mTFP0.7 -H163	3.307	3.601	3.500	2.866	3.080	3.013
mTFP0.7 -N63	3.268	3.731	3.594	2.862	3.115	3.037
mTFP0.7 -H197	3.264	3.767	3.636	2.850	3.113	3.039

S4 Molecular electrostatic field

Table S8: Component of electrostatic field parallel to $\Delta\vec{\mu}$, $F_{\parallel}$ (MV/cm). The QM subsystem comprises only the chromophore.

Protein	with CO[‡]				without CO[♯]			
	CAM-B3LYP		CASSCF		CAM-B3LYP		CASSCF	
	$F_{\parallel}^{QM/MM}$	$F_{\parallel}^{GS}$	$F_{\parallel}^{GS}$	$\delta_{\parallel}^{\S}$	$F_{\parallel}^{QM/MM}$	$F_{\parallel}^{GS}$	$F_{\parallel}^{GS}$	$\delta_{\parallel}$
phiYFP	-17.7	-32.0	-32.5	2.4	-3.3	-17.1	-16.6	2.1
EYFP OH^{145} ↑	-20.2	-38.4	-37.5	1.8	-8.7	-25.7	-24.2	1.5
EYFP OH^{145} ↓	-22.0	-40.4	-41.2	3.0	-10.6	-27.5	-27.7	2.6
Dronpa (2iov)	-23.7	-45.9	-50.9	6.7	-5.4	-24.6	-28.9	6.0
Dronpa (2z1o)	-22.3	-39.8	-44.1	6.5	-6.6	-24.0	-28.1	5.4
GFP-S65T OH^{145} ↑	-30.6	-46.6	-51.7	8.7	-18.2	-32.2	-36.4	8.6
GFP-S65T OH^{145} ↓	-33.7	-49.4	-55.1	9.9	-23.8	-36.6	-41.4	9.8
mTFP0.7	-34.5	-52.8	-56.5	13.6	-26.6	-43.7	-46.2	13.0

[‡]Average of $F_{\parallel}$ over non-H atom positions of HBI chromophore including the CO groups
[♯]Average of $F_{\parallel}$ over non-H atom positions of HBI chromophore excluding the CO groups
[§] $\delta_{\parallel} = F_{\parallel}^{ES} - F_{\parallel}^{GS}$ is the field variation in polSS

Table S9: Angle (degrees) between $\Delta\vec{\mu}$ and $\vec{\mu}_{01}$. The QM subsystem consists of the chromophore alone.

Protein	CAM-B3LYP		LC-BLYP		CASPT2		CASPT2 FFPT		
	QM/MM	GS	QM/MM	GS	QM/MM	GS	QM/MM	GS	SS[†]
phiYFP	26.8	4.3	16.1	2.0	41.7	12.9	45.4	17.8	17.2
EYFP OH^{145} ↑	24.4	1.7	21.5	5.0	14.7	12.9	15.4	10.9	10.5
EYFP OH^{145} ↓	15.3	1.8	5.6	4.3	15.0	8.2	-	9.8	8.3
Dronpa (2iov)	3.5	3.6	5.9	4.0	19.6	5.5	-	7.3	5.5
Dronpa (2z1o)	1.0	2.8	4.8	3.6	18.9	6.3	10.5	8.1	6.4
GFP-S65T OH^{145} ↑	2.7	4.7	2.9	4.8	9.9	3.6	10.9	8.5	6.4
GFP-S65T OH^{145} ↓	1.5	4.9	3.1	4.6	6.8	3.5	8.8	8.4	6.2
mTFP0.7	2.0	4.7	3.1	4.3	4.7	3.0	6.9	6.4	5.9

[†] Angle between $\vec{\mu}_{01}^{\text{polGS}}$ and $\Delta\vec{\mu}^{\text{polSS}}$.

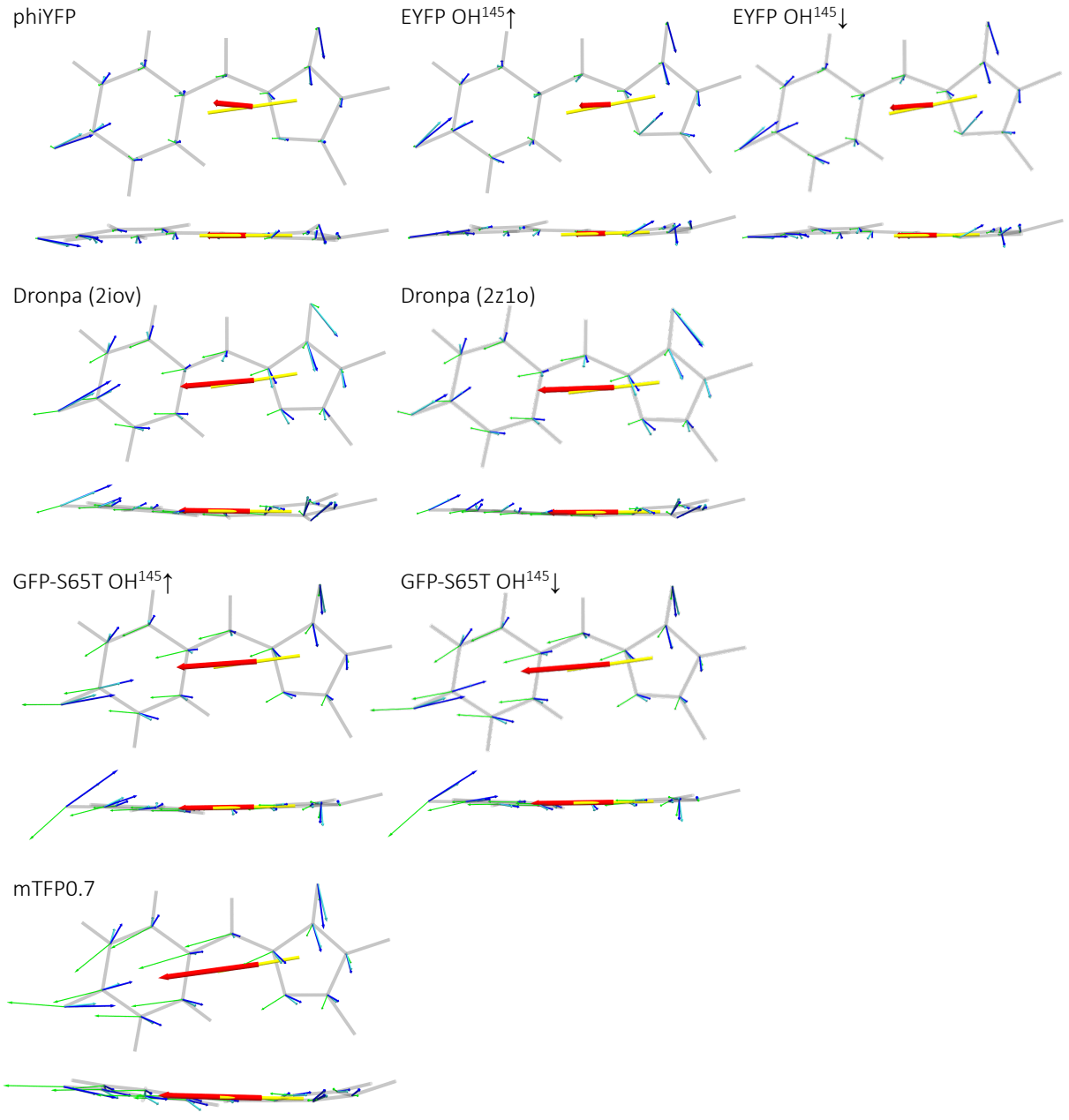

Figure S8: Electrostatic field on the chromophore atoms computed within QM/MM ($\vec{F}^{\mathrm{QMMM}}$, cyan arrows) and polGS ($\vec{F}^{\mathrm{polGS}}$, blue arrows). The variation of polarisation field upon excitation (i.e. the difference between the ground and excited states in polSS) is denoted as $\vec{\delta} = \vec{F}^{\mathrm{polES}} - \vec{F}^{\mathrm{polGS}}$ (green arrows) and scaled up ten times for ease of visualisation. Red arrows and yellow cylinder are respectively $\Delta\mu^{\mathrm{polGS}}$ (CASPT2 FFPT) and μ_{01}. In all cases, the data refer to calculations employing only the chromophore as QM subsystem.

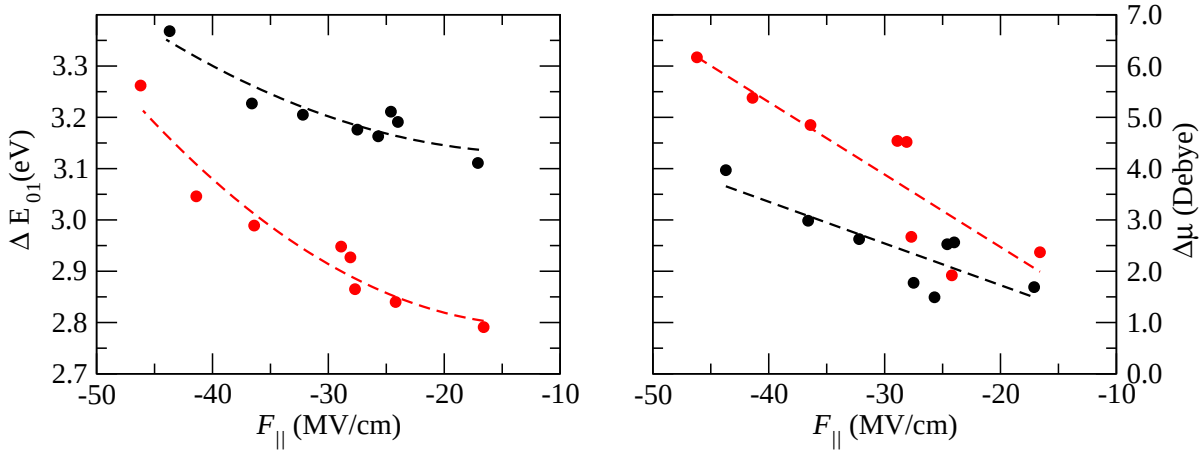

Figure S9: $\Delta E_{01}^{\mathrm{polGS}}$ excitation energy (left) and $\Delta\mu^{\mathrm{polGS}}$ (right) as a function of $F_{\parallel}^{\mathrm{polGS}}$ in CAM-B3LYP (black circles) and CASPT2 (red circles). The value $F_{\parallel}^{\mathrm{polGS}}$ is the average over the chromophore atoms excluding the two CO groups ("without CO" in Table S8). The CASPT2 $\Delta\mu^{\mathrm{polGS}}$ values are from a FFPT calculation.

One way to estimate the molecular field inside GFP was worked out in Ref.,[S1] based on the value of the (measured) $|\Delta\mu|$ in different proteins. In a *static* field $\vec{F}$, one has in the linear regime:

$$\Delta\vec{\mu}(\vec{F}) = \Delta\vec{\mu}^{vac} + \Delta\alpha^{vac} \cdot \vec{F}\,, \tag{S4}$$

where $\Delta\alpha = \alpha_1 - \alpha_0$ is the variation of the polarisability tensor upon excitation and the *vac* superscript identifies quantities *in vacuum* (one can actually employ a different reference system and, in that case, the field variation from the reference is measured). Hence, approximating the problem as unidimensional, an effective field can be estimated by inverting this equation and using for $\Delta\alpha^{vac}$ and $\Delta\mu^{vac}$ values from experiment or from theory.

Calling $\vec{F}^{\rm polGS}$ and $\vec{F}^{\rm polSS}$ the local electric fields in the chromophore cavity (in our MMpol model these are due to the MM charges and dipoles) in the excited and ground state respectively, one has

$$\mu_0^{\rm polGS} = \mu_0^{vac} + \alpha_0^{vac} \cdot \vec{F}^{\rm polGS},\ \ \mu_1^{\rm polES} = \mu_1^{vac} + \alpha_1^{vac} \cdot \vec{F}^{\rm polES} \tag{S5}$$

$$\Delta\vec{\mu}^{\rm polSS} = \vec{\mu}_1^{\rm polES} - \vec{\mu}_0^{\rm polGS} = \Delta\vec{\mu}^{vac} + \Delta\alpha^{vac} \cdot \vec{F}^{\rm polGS} + \alpha_1^{vac} \cdot \vec{\delta} \tag{S6}$$

$$\Delta\vec{\mu}^{\rm polSS} = \Delta\vec{\mu}^{\rm polGS} + \alpha_1^{vac} \cdot \vec{\delta}\,, \tag{S7}$$

where $\vec{\delta} = \vec{F}^{\rm polES} - \vec{F}^{\rm polGS}$ is the (reaction) field variation due to the different environment polarisation (i.e. different set of MM dipoles in the excited state and in the ground state) and α_1 refers to excited-state polarisability. The $\vec{\delta}$s for the various proteins are reported in Fig.S8, together with $\vec{F}^{\rm polGS}$ and the vectors corresponding to $\Delta\mu$ and μ_{01}, showing that, though not perfectly parallel, $\vec{\delta}$ is roughly in the same direction as $\Delta\vec{\mu}$ (in GFP-S65T there is a strong component perpendicular to the chromophore plane, in the phenolate carbonyl).

In first-order perturbation theory and ignoring inhomogeneity, it should be $\vec{\delta}\cdot\Delta\vec{\mu}^{\rm polGS} = g_e(\Delta\mu^{\rm polGS})^2$, and, considering $\vec{\delta}$ and $\Delta\vec{\mu}^{\rm polGS}$ parallel, it is $\delta \simeq g_e\Delta\mu^{\rm polGS}$. The measured $\Delta\mu$, i.e. $\Delta\mu^{\rm polSS}$, can then be related to $\Delta\mu^{\rm polGS}$ and $F_{||}^{\rm polGS}$ through

$$\Delta\mu^{\rm polSS} = (1 + \alpha_1^{vac} g_e)\Delta\mu^{\rm polGS} \tag{S8}$$

$$\tag{S9}$$

$F_{||}^{\rm polGS}$ can thus still be recovered:

$$F_{||}^{\rm polGS} = \frac{(1 + \alpha_1^{vac} g_e)^{-1}\Delta\mu^{\rm polSS} - \Delta\mu^{vac}}{\Delta\alpha^{vac}}. \tag{S10}$$

Overall the correction with respect to the use of Eq.S4 is moderate, because from our data we have $\Delta\mu^{\rm polSS} \simeq 1.1\Delta\mu^{\rm polGS}$, and their direction is virtually the same. From $\alpha_1^{vac} g_e \simeq 0.1$, we get an estimate

of $\alpha_1 \simeq 30$ Å^3 when our value for g_e is plugged into the equation.

We note however that, in order to reproduce the measured $\Delta\mu$ (Table 3 in the main text), we also include the contribution from the changing dipoles of the embedding. Therefore, there is an additional rescaling of the experimental $\Delta\mu^{\text{exp}}$ in Eq. S10 so that we have

$$F_{||}^{\text{polGS}} = \frac{\eta\Delta\mu^{\text{exp}} - \Delta\mu^{vac}}{\Delta\alpha^{vac}}, \tag{S11}$$

where, from our data, $\eta \sim 1.2$.

References

(S1) Drobizhev, M.; Callis, P. R.; Nifosì, R.; Wicks, G.; Stoltzfus, C.; Barnett, L.; Hughes, T. E.; Sullivan, P.; Rebane, A. Long- and Short-Range Electrostatic Fields in GFP Mutants: Implications for Spectral Tuning. *Scientific Reports* **2015**, *5*, 13223.